AD-A264 411

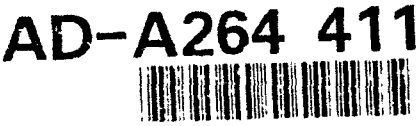

FR-60256

A Final Report for:

MULTI-QUANTUM WELL LATERAL-FIELD-EFFECT ELECTRO-REFRACTION MODULATOR

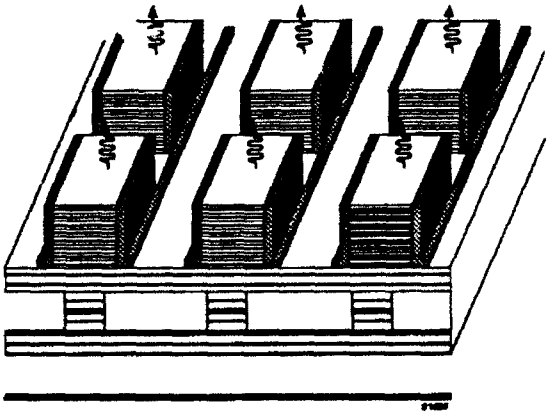

DTIC
ELECTE
MAY 14 1993
S B D

Report period:
August 10, 1992 - March 30, 1993

Submitted under:
Contract Number N00014-92-C-0150

Submitted to:
OFFICE OF NAVAL RESEARCH
Department of the Navy
800 N. Quincy Street Code 1511:RD
Arlington, VA 22217-5000

DISTRIBUTION STATEMENT A
Approved for public release;
Distribution Unlimited

93-10643

spire

FR-60256

A Final Report for:

MULTI-QUANTUM WELL LATERAL-FIELD-EFFECT ELECTRO-REFRACTION MODULATOR[1]

Report period:

August 10, 1992 - March 30, 1993

Submitted under:

Contract Number N00014-92-C-0150

Submitted to:

OFFICE OF NAVAL RESEARCH

Department of the Navy

800 N. Quincy Street Code: 1511:RD

Arlington, VA 22217-5000

Submitted by:

Spire Corporation

One Patriots Park

Bedford, MA 01730-2396

---

[1] Research is sponsored by SDIO/IST and managed by Office of Naval Research.

REPORT DOCUMENTATION PAGE

Form Approved
OMB No 0704-0188

Public reporting burden for this collection of information is estimated to average 1 hour per response, including the time for reviewing instructions, searching existing data sources, gathering and maintaining the data needed, and completing and reviewing the collection of information. Send comments regarding this burden estimate or any other aspect of this collection of information, including suggestions for reducing this burden, to Washington Headquarters Services, Directorate for Information Operations and Reports, 1215 Jefferson Davis Highway, Suite 1204, Arlington, VA 22202-4302, and to the Office of Management and Budget, Paperwork Reduction Project (0704-0188), Washington, DC 20503.

1. AGENCY USE ONLY *(Leave blank)*	2. REPORT DATE	3. REPORT TYPE AND DATES COVERED
	May 7, 1993	Final August 10, 1992 - March 30, 1993

4. TITLE AND SUBTITLE
MULTI-QUANTUM WELL LATERAL-FIELD-EFFECT ELECTRO-REFRACTION MODULATOR

5. FUNDING NUMBERS
N00014-92-C-0150

6. AUTHOR(S)
H. Paul Maruska, Ph.D.

7. PERFORMING ORGANIZATION NAME(S) AND ADDRESS(ES)
Spire Corporation
One Patriots Park
Bedford, MA 01730-2396

8. PERFORMING ORGANIZATION REPORT NUMBER
FR-60256

9. SPONSORING/MONITORING AGENCY NAME(S) AND ADDRESS(ES)
Strategic Defense Initiative Organization
The Pentagon, Washington, DC
Office of Naval Research, 800 North Quincy Street
Arlington, VA 22117-5000

10. SPONSORING/MONITORING AGENCY REPORT NUMBER

11. SUPPLEMENTARY NOTES

12a. *DISTRIBUTION/AVAILABILITY STATEMENT*
Approved for public release; distribution unlimited

12b. DISTRIBUTION CODE

13. ABSTRACT *(Maximum 200 words)*

We have successfully designed, fabricated, and tested a new electro-optic modulator based on the Lateral Electric Field Induced Refraction (LEFIR) effect. The entire combination of GaAs and $Al_xGa_{1-x}As$ layers, including multiple quantum wells and delta-doped planes, were deposited by metalorganic chemical vapor deposition in a single growth run. The modulator was fashioned as a tunable Fabry-Perot Interferometer, with upper and lower stacks of Bragg mirrors enclosing the active spacer region, which contains the quantum wells. It was shown that the basic operating principle for the LEFIR modulator relies on shifting electric charges, which originated in the delta-doped plane, into and out of the series of quantum wells, i.e., the Band Filling Electro-Optic Effect. After successful deposition of individual mirrors, delta-doped planes, and quantum well structures, a complete LEFIR modulator was produced, which exhibited a sharp Fabry-Perot transmission mode at 969 nm. Calculations indicated that the transmission of the device can be shifted from 75% to 5% by the application of about 15 volts bias with the initial structure. In Phase II, we shall seek to optimize the structure, and to progress to two-dimensional arrays of modulators.

14. SUBJECT TERMS
Electro-optic modulator, Fabry-Perot Interferometer, Band-filling electro-refraction, multiple quantum wells.

15. NUMBER OF PAGES
33

16. PRICE CODE

17. SECURITY CLASSIFICATION OF REPORT	18. SECURITY CLASSIFICATION OF THIS PAGE	19. SECURITY CLASSIFICATION OF ABSTRACT	20. LIMITATION OF ABSTRACT
Unclassified	Unclassified	Unclassified	UL

ABSTRACT

We have successfully designed, fabricated, and tested a new electro-optic modulator based on the Lateral Electric Field Induced Refraction (LEFIR) effect. The entire combination of GaAs and $Al_xGa_{1-x}As$ layers, including multiple quantum wells and delta-doped planes, were deposited by metalorganic chemical vapor deposition in a single growth run. The modulator was fashioned as a tunable Fabry-Perot Interferometer, with upper and lower stacks of Bragg mirrors enclosing the active spacer region, which contains the quantum wells. It was shown that the basic operating principle for the LEFIR modulator relies on shifting electric charges, which originated in the delta-doped plane, into and out of the series of quantum wells, i.e., the Band Filling Electro-Optic Effect. After successful deposition of individual mirrors, delta-doped planes, and quantum well structures, a complete LEFIR modulator was produced, which exhibited a sharp Fabry-Perot transmission mode at 969 nm. Calculations indicated that the transmission of the device can be shifted from 75% to 5% by the application of about 15 volts bias with the initial structure. In Phase II, we shall seek to optimize the structure, and to progress to two-dimensional arrays of modulators.

Accession For
NTIS GRA&I ☑
DTIC TAB ☐
Unannounced ☐
Justification
By
Distribution /
Availability Codes
Dist | Avail and/or Special
A-1

TABLE OF CONTENTS

LIST OF ILLUSTRATIONS

LIST OF ILLUSTRATIONS (Concluded)

LIST OF TABLES

1 INTRODUCTION AND BACKGROUND

1.1 Statement of Problem

High-speed electro-optic components, fabricated from III-V compound semiconductors exhibiting nonlinear optical effects, offer great promise for relieving bottlenecks in critical areas of optical signal processing as applied to defense department needs in communications, optical interconnects, and optical computing/logic applications. Particularly vital to these efforts are the development of temporal and spatial light modulators. We propose a new design for a modulator based on GaAs technology, which operates on the principle of changing the refractive index of a device by sweeping out an electron gas from a quantum well. Electrons are filled into the quantum layer from a nearby planar source and swept out by an electric field applied parallel to the grown layers. The applied electric field provides a phase shift for light passing through the device perpendicular to the grown layers, and tunes the reflectivity if the layers are configured as a Fabry-Perot etalon. A single device is an intensity modulator, while an array can accomplish spatial modulation of light.

1.2 Electro-refraction

A phase or amplitude modulator element which can control the propagation characteristics of a lightwave can be attained in a device which changes the absorption constant and the refractive index of the material. Generally, this task is accomplished by applying an electric field to the sample. There are four major effects due to the application of this field, two of which are direct consequences of the field, and two of which are due to either the addition or the removal of free carriers by the field.[1] (i) The Linear Electrooptic Effect (Pockels Effect) results from birefringence induced by a filed applied to a non-centrosymmetric material, such as GaAs. The change in refractive index depends on direction of propagation of the lightwave through the crystal. (ii) The Franz-Keldysh Effect occurs due to the tilting of the band edges when the field is applied, which shifts the absorption edge. The shift in absorption will cause a variation in refractive index, based on the Kramers-Kronig relationship. (iii) The Plasma Refraction Effect is due to direct optical absorption by free carriers. These carriers are supplied or removed by the field. (iv) The Band Filling Effect is evidenced by a shift in the absorption edge of the material as the lowest states in the conduction band are filled or emptied by an applied field.

It is expected that the principal electro-refractive effect that will operate in our quantum well modulator will be the Band Filling Effect. The change in refractive index will arise from the change of absorption due to correlated filling or emptying of states in the quantum well. This phenomenon of phase-space absorption modulation is a generalized form of the Moss-Burnstein shift.[2]

1.3 Optical Modulators

The simplest approach for impressing information on the optical output of a diode laser source is to modulate the drive current. This serves to alter the carrier density and hence gain of the laser cavity and therefore to change the emitted optical power from the laser. Unfortunately, the change in carrier density also alters the refractive index as just discussed, leading to undesirable frequency modulation (chirp). However, we can utilize the electro-refractive effects to construct a separate optical modulator capable of either intensity or phase modulation; because

it is placed external to the laser, the modulator will not chirp the laser frequency in an uncontrolled manner.

The optical modulator that we are developing allows light to be incident perpendicular to a stack of grown layers in a semiconductor system such as GaAs/AlGaAs, a basic necessity for two-dimensional arrays.[3] When fabricated in the form of an array of mesas, the electric field is applied transverse across each mesa, parallel to the grown layers: the field is equal along each quantum well layer in a mesa, a condition which is never realized if the field is applied perpendicular to the layers.[4] The quantum wells are not intentionally doped, but are filled with electrons from a nearby plane of dopants (Δ-doped layer). Changing the electron population in each well alters the refractive index, and causes a phase shift. Thus, the Lateral-Electric-Field-Induced-Refraction (LEFIR) effect can be applied to the construction of reflective modulators, and allows beam steering. These LEFIR modulators can easily be extended into two-dimensional arrays, sequentially deposited onto vertical cavity surface-emitting lasers (VCSEL), with applications as self-emissive spatial light modulators (SLM). Thus, our proposed LEFIR modulators can find application both as a single element, monolithically integrated with a VCSEL to provide the intensity modulation function; and as a two-dimensional array of voltage controlled reflectors to provide spatial light modulation.

1.4 LEFIR Modulator Concept

The device concept is shown schematically in Figure 1. The voltage-tunable reflector is fabricated in the form of a Fabry-Perot interferometer, with a set of mirrors grown as quarter wave dielectric stacks[5] with the active region placed between the mirrors. Such mirrors can exhibit reflectivities approaching 100% as the number of layers is increased.[6] The active region contains a series of quantum wells, nominally undoped. The higher bandgap layers between the quantum wells serve as potential barriers that basically restrict any carriers in the wells to two dimensions, parallel to the grown layers. Each barrier has at its center a plane of doped material, a so-called Δ-doped layer.[7,8] It is energetically favorable for these electrons to transfer from the Δ-doped layer into the adjacent quantum well. The presence of the electrons in the quantum well effectively bleaches the absorption that would occur between the lower subbands of the well, which is basically a Moss-Burstein shift.[9] Removal of these electrons from the path of the light will affect both the optical absorption and the refractive index[10], since these two quantities are mutually dependent through the Kramers-Kronig relation.

The application of a lateral electric field, in the direction parallel to the surfaces of the grown layers, will rapidly move the electron population to the side of the structure, out of the path of the light. Since there are no charged impurities in the well, because the electrons were transferred from the Δ-doped layer, carrier motion is expected to be extremely fast, as in a planar-doped MODFET.[11] Net capacitance is lowered because the donor ions and the electrons are separated by the distance of half a barrier layer thickness. Because the device utilizes a change in refractive index rather than absorption as its basis of operation, ideally no photo-generated current will flow, and, therefore, the contacts on either side of the mesa are made blocking by imposing a thin insulating film. This eliminates any dark current from flowing along the device. The insulator is generally an improvement over simple Schottky barriers in restricting current flow, especially since, if the concept is to be extended to InGaAsP/InP materials, functional Schottky contacts would be difficult to implement.[12] In the present manifestation,

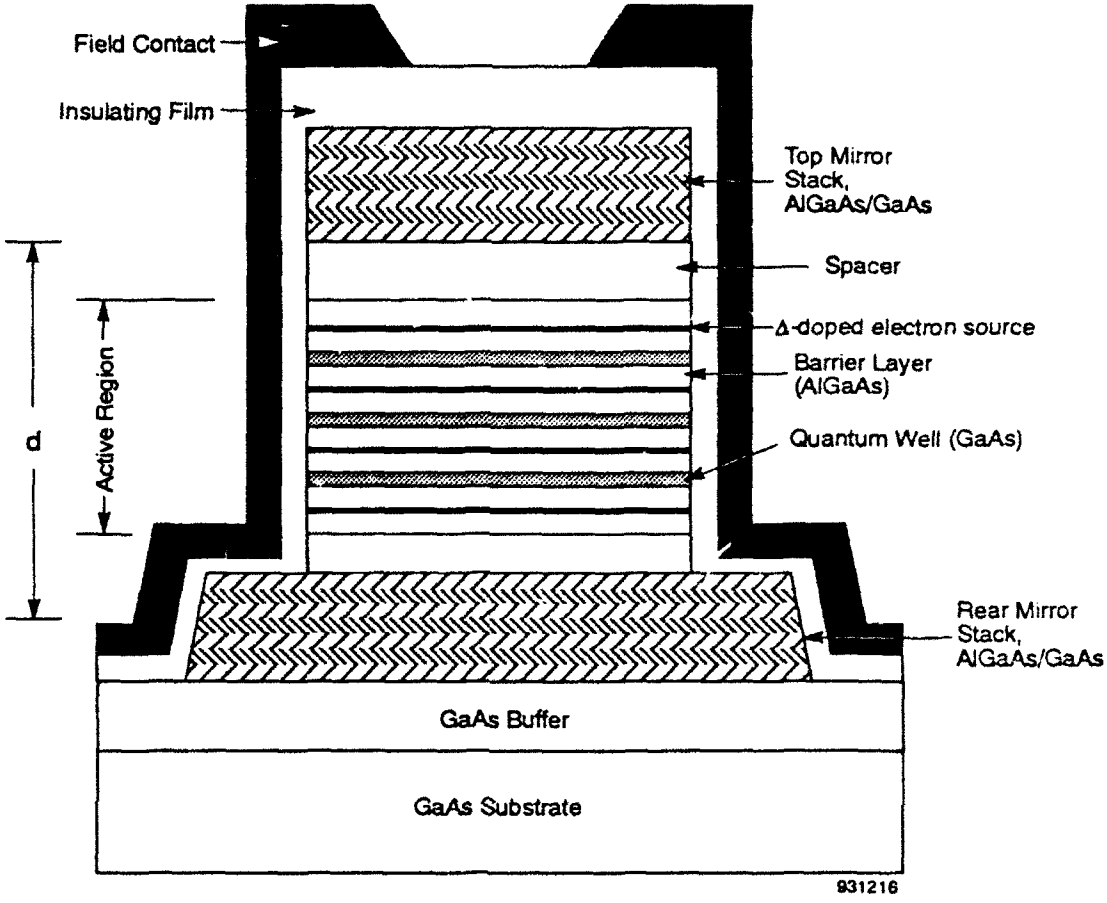

Figure 1 *Structure of lateral electric field induced refraction (LEFIR) modulator.*

the incident light must have a wavelength longer than the absorption edge (excitonic absorption)[13] in the quantum well.

Resonance in the structure is achieved when twice the optical path length, $n_e d$, equals an integral multiple of the wavelength, where d is defined in Figure 1, and n_e is the effective refractive index of the active region. At resonance, the reflectance of the structure approaches zero, and the width of this transmission band depends on the finesse or, basically, on the magnitude of the reflectivity of each mirror. Very high reflectivity mirrors are desirable to insure a very narrow passband, and hence a very large change in reflection, as n_e is altered by the external field. This insures high contrast and, hence, strong intensity modulation for the structure.

By vertically integrating the LEFIR elements with an array of VCSEL's, it will be possible to provide beam steering of the combined diode laser output beam for direct laser communications between satellites. That is, the phase of the emission of each laser in the array

can be individually controlled by an external electrical signal. In this configuration, the LEFIR's would not be utilized in the Fabry-Perot interferometer mode but, instead, as phase shifters to control each optical beam. The induced phase shift can be written as,

$$\Phi = (2\pi d/\lambda)\Delta n_e \qquad (1)$$

Thus, if λ = 0.9 μm, d = 3 μm, and Δn_e = 0.3, then a phase shift of 2π would be possible. Figure 2 indicates this type of array.

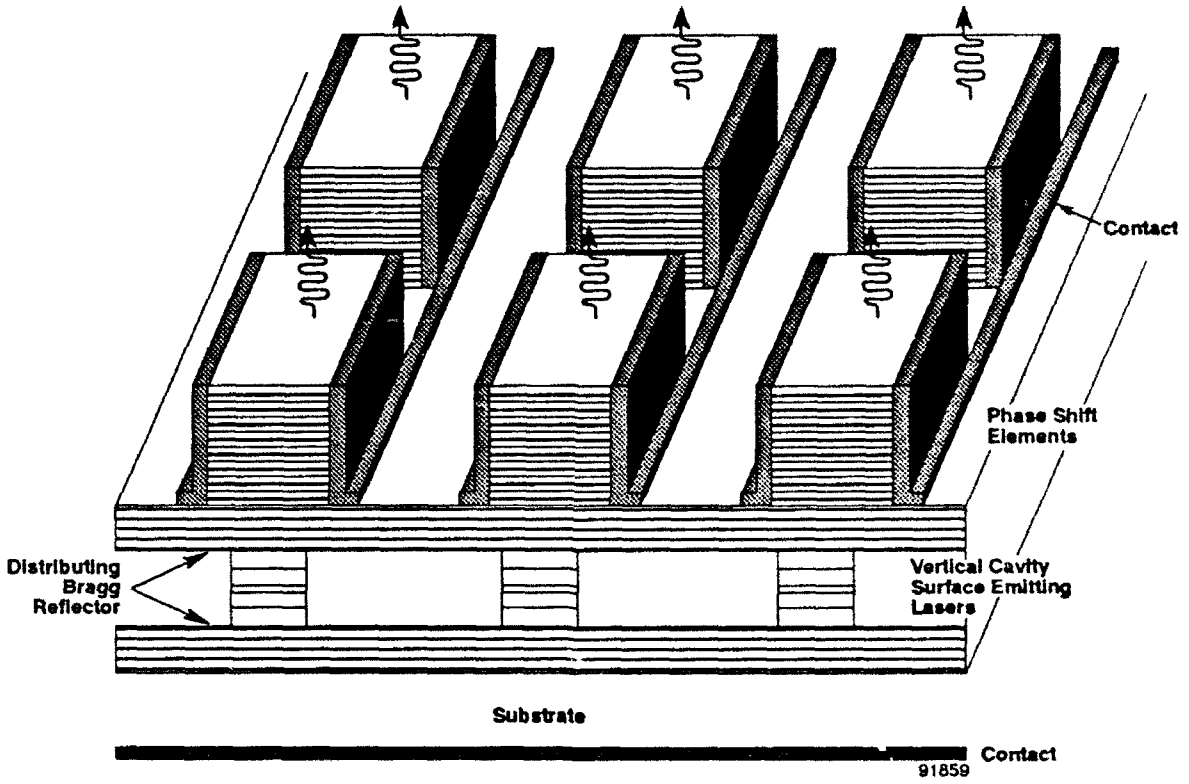

Figure 2 *Application of LEFIR phase shift elements to provide beam control for two-dimensional array of vertical cavity surface emitting lasers.*

The basic operation of the proposed device can be illustrated as follows. The desired phase shift is controlled through an externally tunable density of free electrons in a quantum well, which linearly changes the refractive index.[14] Figure 3(a) indicates that with no lateral field applied, the device has a certain refractive index due to the presence of the electron gas, which fills all possible receiving states in the quantum well. When the applied field clears the states (Figure 3(b)), by moving the electrons laterally, the refractive index of the structure will be effectively increased, inducing a phase delay for transverse optical signals. The magnitude of the effect is clearly demonstrated in Figure 4, which shows the change in refractive index Δn of GaAs as minority carriers are injected.[15] Note that $|\Delta n| > 0.02$ is possible, according to Figure 4.

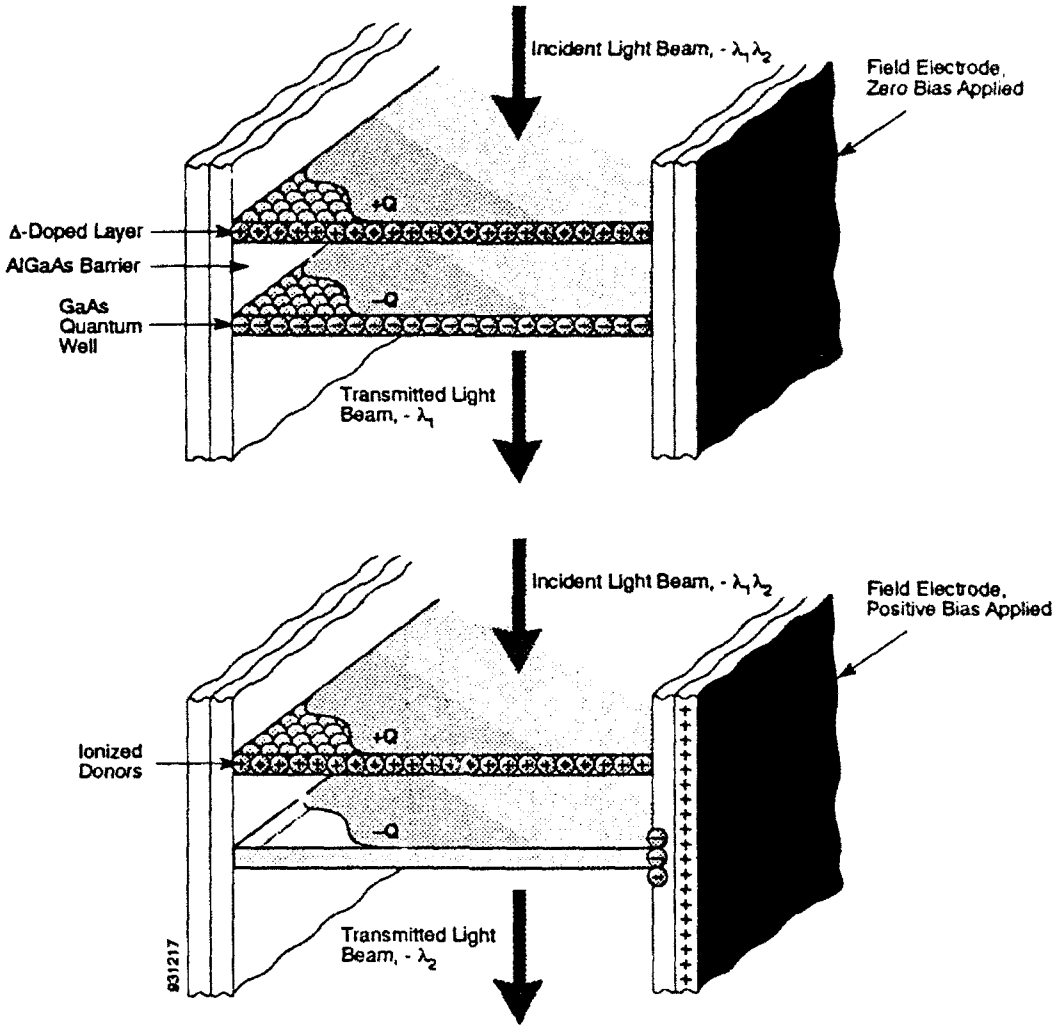

Figure 3 *(a) Quantum well states filled from external source of electrons; (b) clearing of states by lateral electric field.*

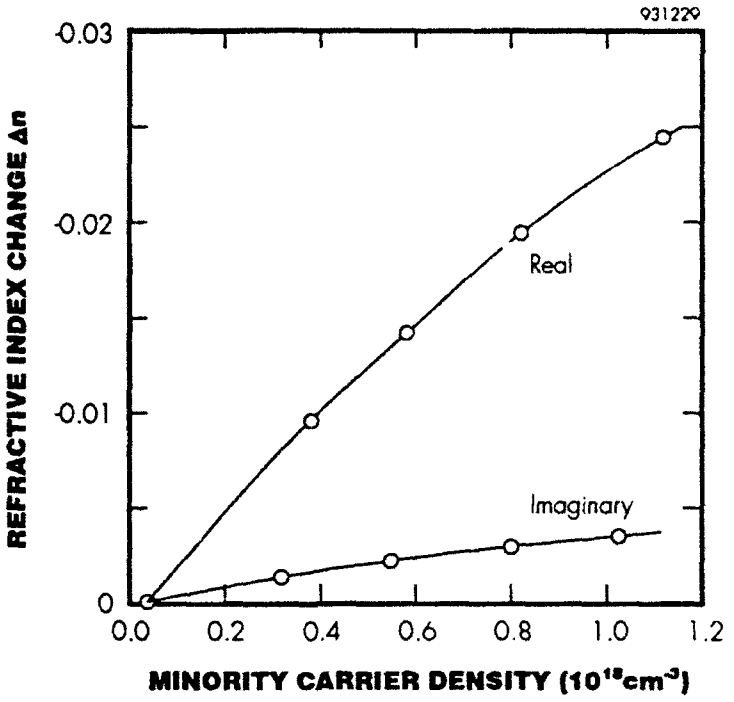

Figure 4 *Changes in the real and the imaginary components of the refractive index of GaAs due to the introduction of free carriers.*

1.5 Other Electro-refractive Modulators

An electro-refraction effect has been previously demonstrated in an alternative structure in which both the light and the electric field were applied transverse to the planes of the grown layers.[16] In the reported device,[16] the electrons were transferred from a heavily-doped barrier into the quantum well when the field was applied across all of the layers, similar to the gate voltage in FET. The anticipated problems are that the field will not be uniform across each QW unit in the stack, that the heavily doped barrier can contribute to insertion loss through free carrier absorption, and that the required placement of the electrodes makes integration with VCSEL's a challenging situation.[17] Our new design is expected to overcome all of these difficulties.

2 PHASE I TECHNICAL OBJECTIVES

The objectives and structure of the proposed research program are defined by the following list of tasks:

Task 1 - Baseline design of lateral-electric-field-induced-refraction (LEFIR) phase-shift modulator: material structure and device configuration.

Task 2 - Growth and characterization of multi-quantum well test structure.

Task 3 - Growth and characterization of distributed Bragg mirror stack.

Task 4 - Growth and characterization of Δ-doped barrier structure.

Task 5 - Fabrication and initial characterization of LEFIR modulator device.

Task 6 - Assessment of problem areas and definition of directions for Phase II effort.

These tasks are designed to provide insight for understanding the functioning of the completed device and to aid in determining the feasibility of the proposed innovation. Specific questions that require addressing include:

- Do the individual sections (mirrors, quantum wells, dopant reservoir, *etc.*) of the overall structure each possess the required properties?
- Under zero-bias conditions, how does the reflectance of the completed structure vary with wavelength of incident light, and how highly peaked is the response of this Fabry-Perot interferometer?
- How strongly does the application of a lateral electric field affect the reflectivity spectrum of the device?

3 PHASE I RESULTS AND DISCUSSION

This section describes the details of the technical effort which successfully accomplished the objectives; *viz.*, to provide a preliminary design for the structure, to fabricate and test individual sections, and to assemble the complete structure with initial evaluation of its properties.

3.1 Task 1 - Baseline Design of LEFIR Phase-Shift Modulator: Material Structure and Device Configuration

The basic structure of the LEFIR modulator was shown in Figure 1. We started with a semi-insulating GaAs substrate and all layers were grown by MOCVD.

The first set of layers will form the lower mirror for the etalon. This Bragg reflector was initially designed to provide a passband centered at 900 nm. The two materials for the quarter wave stack were chosen to be $Al_{0.10}Ga_{0.90}As$, with n = 3.54, and $Al_{0.85}Ga_{0.15}As$, with n = 3.035. To achieve a center wavelength of 900 nm (which will pass through the GaAs substrate), it is required that,

$$\lambda_0/4 = n_1 t_1 = n_2 t_2 \qquad (2)$$

Therefore, we calculated that t_1 = 635Å and t_2 = 740Å. The calculated reflectance *vs.* number of periods in the mirror is shown in Figure 5. We chose to give the mirror 15 periods, which should give a reflectance of 98%. The structure of the mirror is shown in Figure 6. It is clear that a complete LEFIR modulator element must have two sets of Bragg mirrors.

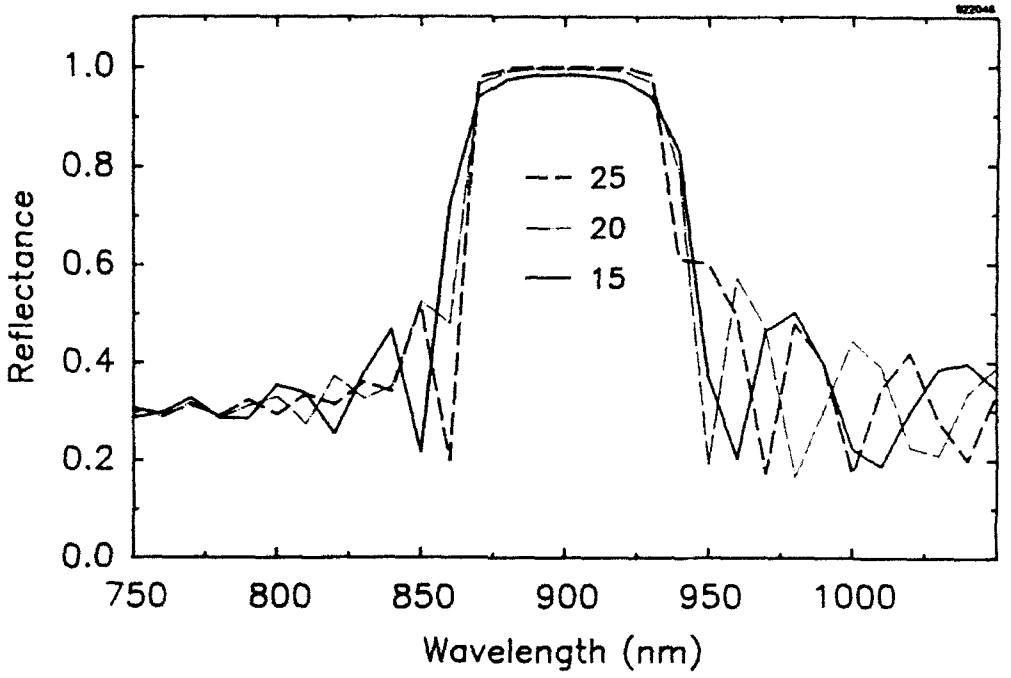

Figure 5 *Calculated Bragg mirror reflectance for 15, 20, and 25 periods of $Al_{0.10}Ga_{0.90}As$/ $Al_{0.85}Ga_{0.15}As$.*

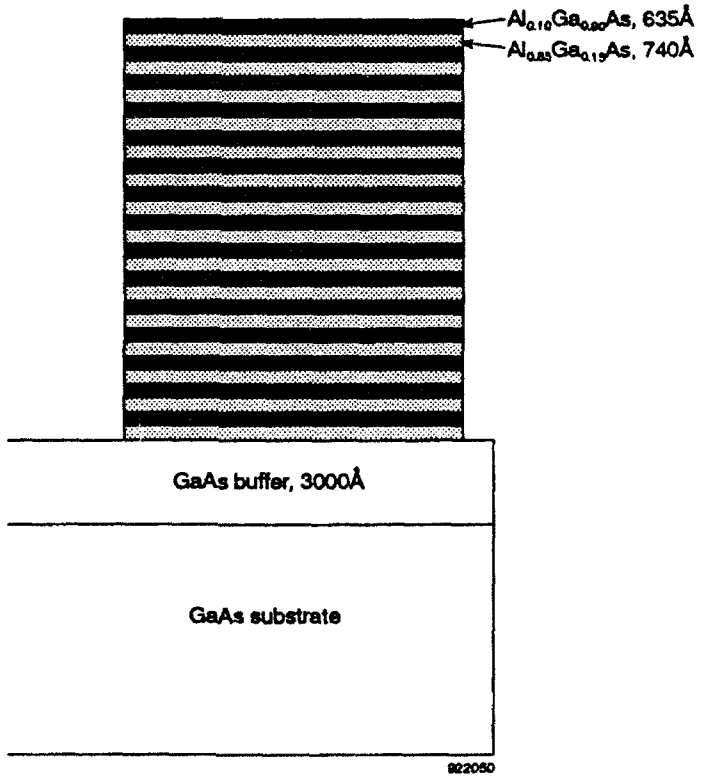

Figure 6 *Configuration of mirror stack grown by MOCVD.*

To create a fixed, non-tunable etalon, a GaAs spacer layer can be grown between the mirror stacks. For a fully functional device, the series of quantum wells and barriers comprising the active region of the Fabry-Perot etalon will be grown. It will contain 100Å GaAs (n = 3.6) quantum wells, and 200Å $Al_{.23}Ga_{.77}As$ (n = 3.4) barriers. The Fabry-Perot resonances can be found to zeroth order from,

$$\lambda_m = \frac{2}{m}[N(3.6)(.01) + (N+1)(3.4)(.02)] = \frac{14.696}{m} \quad (3)$$

where N is the number of quantum wells. We have chosen N to be 70, which implies 71 barrier layers, the first of which serves as the spacer layer. Figure 7 shows the expected resonances. Note that equation (3) is only a rough approximation as it neglects the phase shifts in the mirrors. Our calculated results shown in Figure 7 take the phase shifts in the mirrors into account.

The sheet concentration of dopants introduced into the n-type Δ-doped layer must correspond to the number of sub-band states in the quantum well, basically about 1 x 10^{12} cm^{-2}. Thus, the Δ-doped layer is expected to become completely depleted. Our analysis indicates that the band structure of the unit can be represented as shown in Figure 8. With no bias applied, the quantum well will have the lowest sub-band states filled, and the refractive index will be at its minimum.

Figure 9 is a detailed schematic of the tunable Fabry-Perot interferometer designed in Task 1. The entire structure was eventually grown in a single MOCVD run.

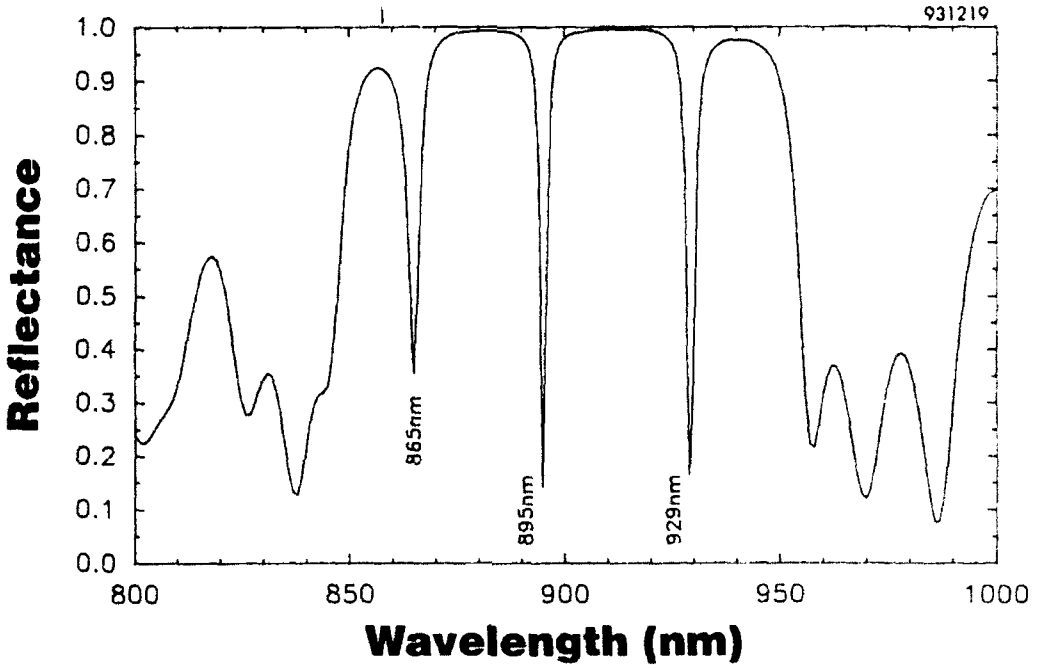

Figure 7 *Calculated spectrum of Fabry-Perot interferometer showing expected resonances.*

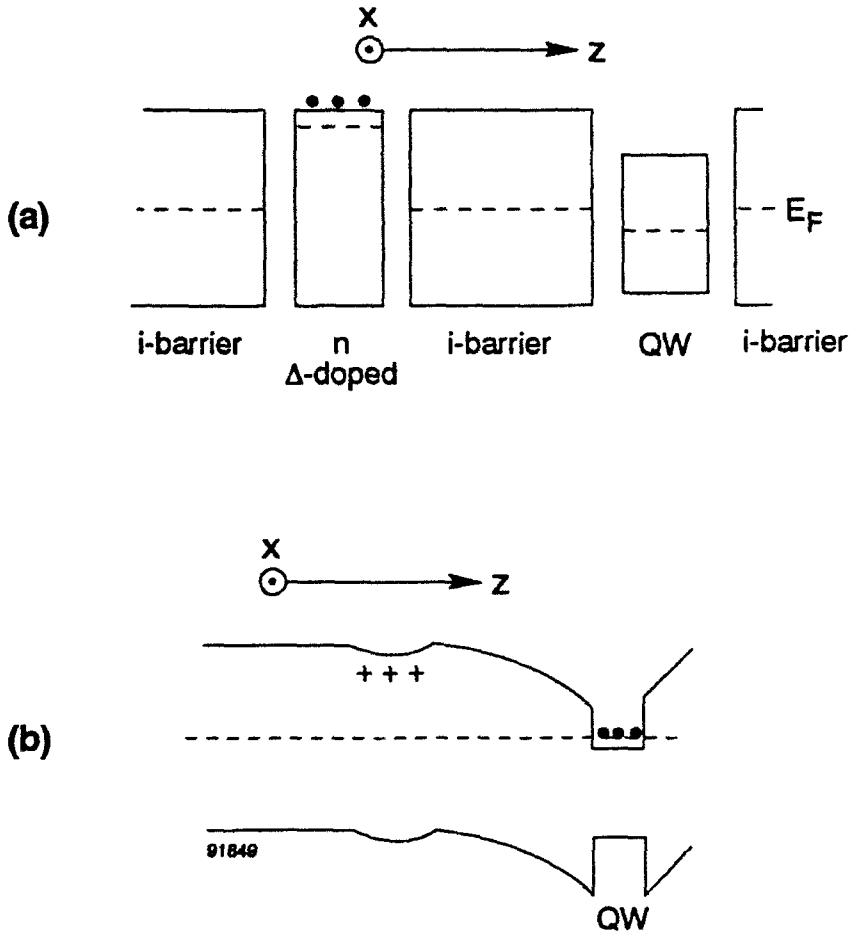

Figure 8 *(a) Fermi level position of individual layers; (b) energy levels of structure at equilibrium.*

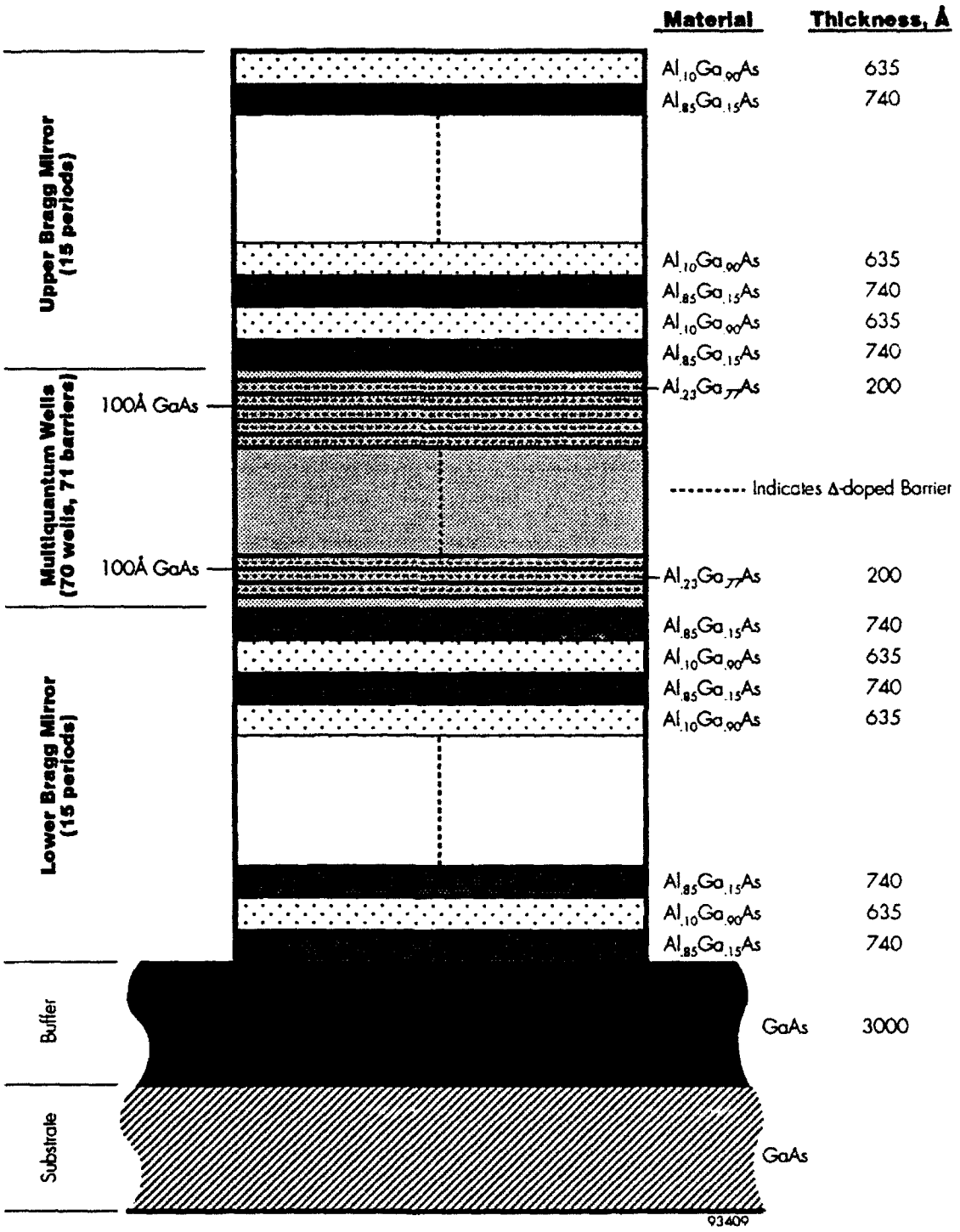

TUNABLE FABRY-PEROT INTERFEROMETER

Figure 9 *Tunable Fabry-Perot interferometer structure.*

3.2 Task 2 - Growth and Characterization of Multi-quantum Well Test Structure

The test structure for calibrating the active region was to comprise the sequence of 70 GaAs quantum wells, each 100Å thick, and 71 $Al_{0.23}Ga_{0.77}As$ barrier layers, each 200Å thick but lacking the Δ-doped plane. Fortunately, rapid progress in parallel programs provided the requisite calibration and characterization data for this task. Figures 10 through 12 illustrate that our MOCVD-grown interfaces are essentially planar and parallel, which is vital for achieving high finesse in the etalon; they also indicate the extraordinary control of period thickness/ uniformity. Since Task 2, as proposed, was superfluous, it was eliminated in favor of devoting more effort to the modulator fabrication of Task 5.

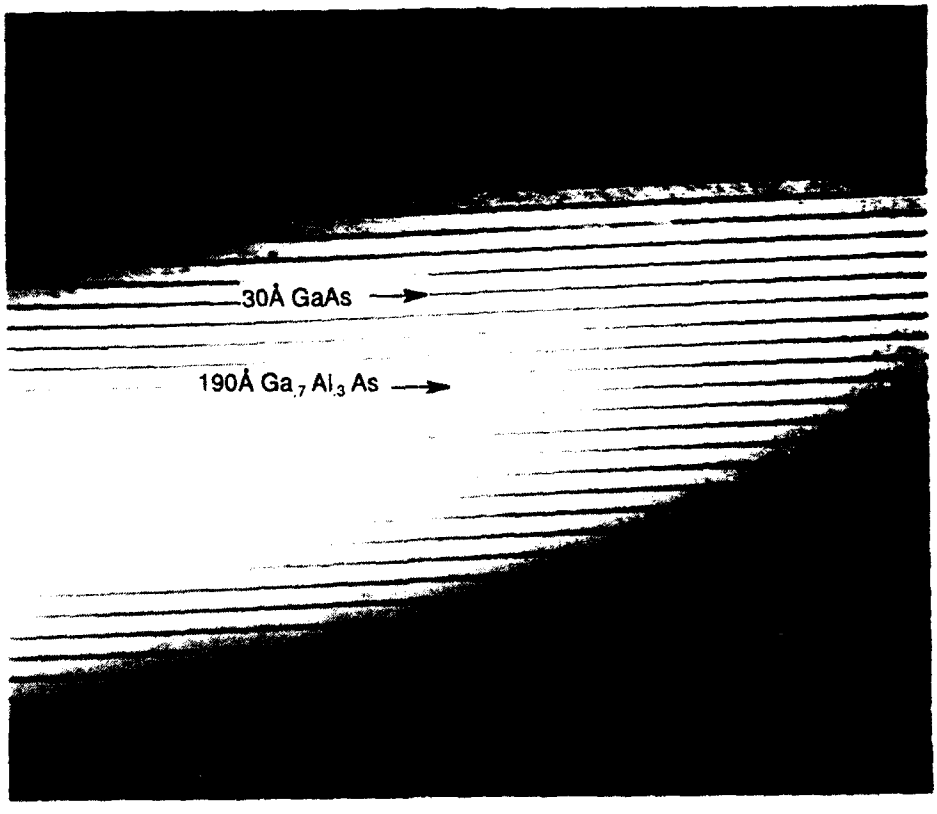

Figure 10 *Cross-section TEM of GaAs - GaAlAs 50 - period superlattice grown at Spire by LP-MOCVD.*

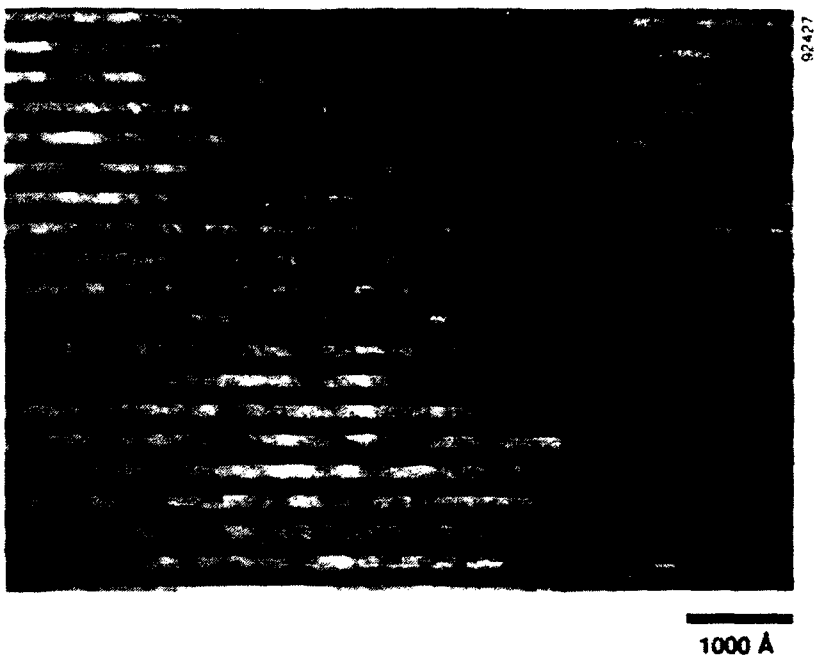

Figure 11 *XTEM showing portion of 100-period InP-InGaAs superlattice.*

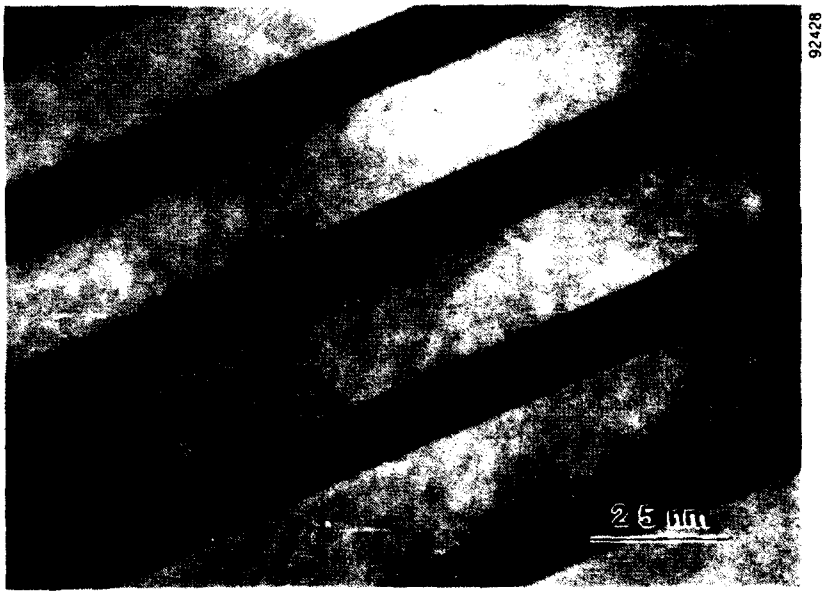

Figure 12 *XTEM showing portion of 100-period InP-InGaAs superlattice at high magnification.*

3.3 Task 3 - Growth and Characterization of Distributed Bragg Mirror

The 15-period mirror stacks were grown in a SPI-MOCVD™ 450 reactor, at 720°C, at a reactor pressure of 76 torr and a V/III ratio of 90:1. The mirrors were characterized mainly by Optical Reflectance Spectroscopy. The first Bragg reflector grown had too short a passband wavelength (peak transmission at 800 nm), because the layers were too thin, being 560Å and 600Å for $Al_{0.10}Ga_{0.90}As$ and $Al_{0.85}Ga_{0.15}As$, respectively. However, its photoluminescence spectrum confirmed the composition. As shown in Figure 13, the peak at 790 nm indicates an aluminum concentration of 9.8%, which compares quite favorably with our requirement of 10%. The second Bragg reflector that we grew did achieve the desired passband, as shown in Figure 14. The peak transmission is at 920 nm. The layer thicknesses were verified by REFIT analysis of the optical data.

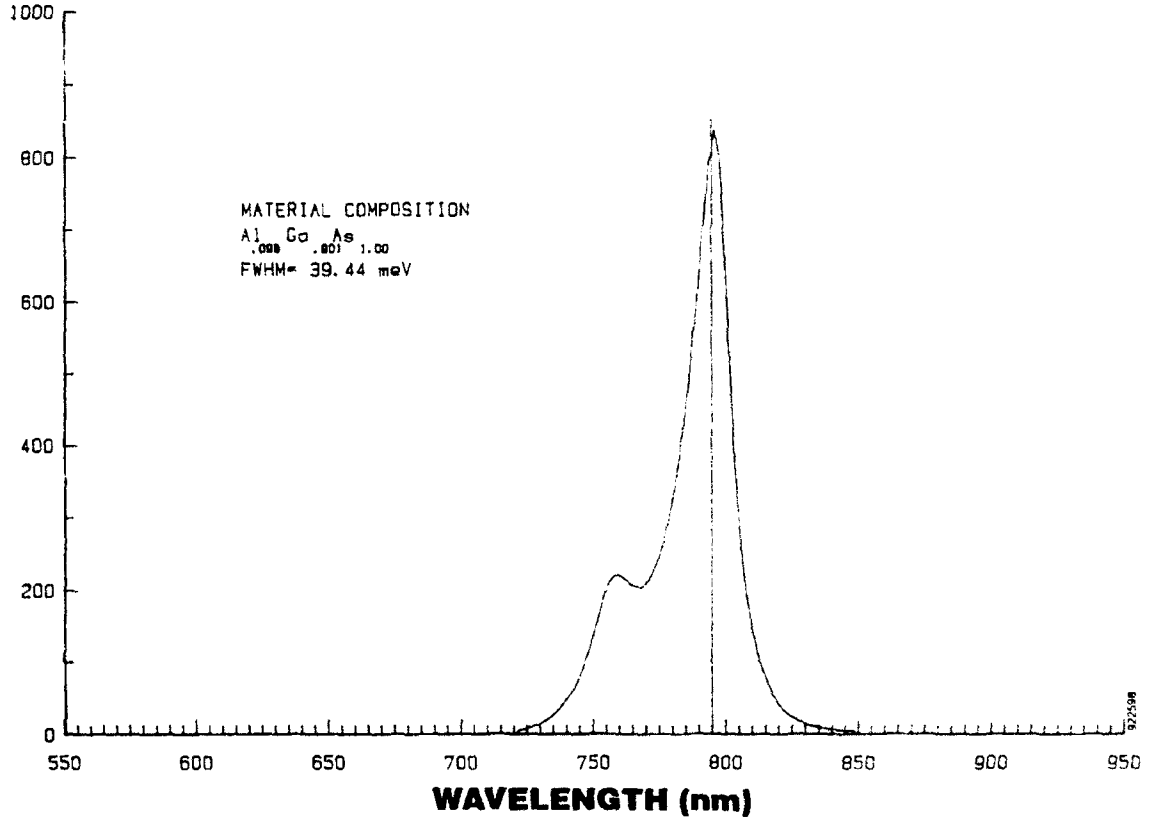

Figure 13 *Photoluminescence spectrum of Bragg mirror.*

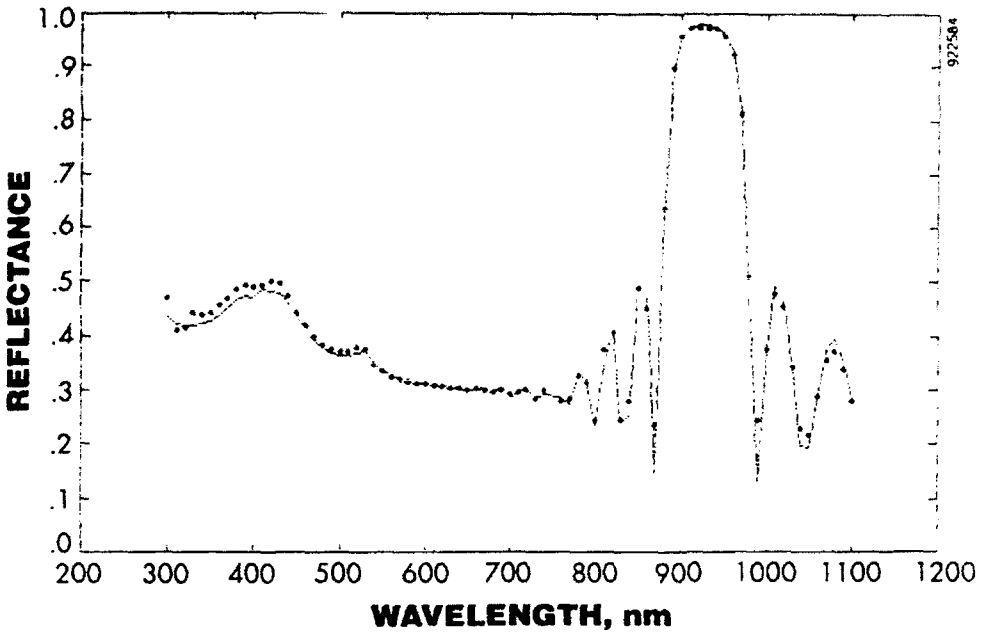

Figure 14 *Transmission spectrum of Bragg mirror.*

3.4 Task 4 - Growth and Characterization of Δ-Doped Structure

The test structure for Δ-doping was a single barrier layer with one heavily Si-doped, nominally single plane (monolayer), deposited on a semi-insulating GaAs substrate. See Figure 15. For convenience in characterization, a total AlGaAs thickness of 400 nm was grown. The deposition conditions are enumerated in Table I.

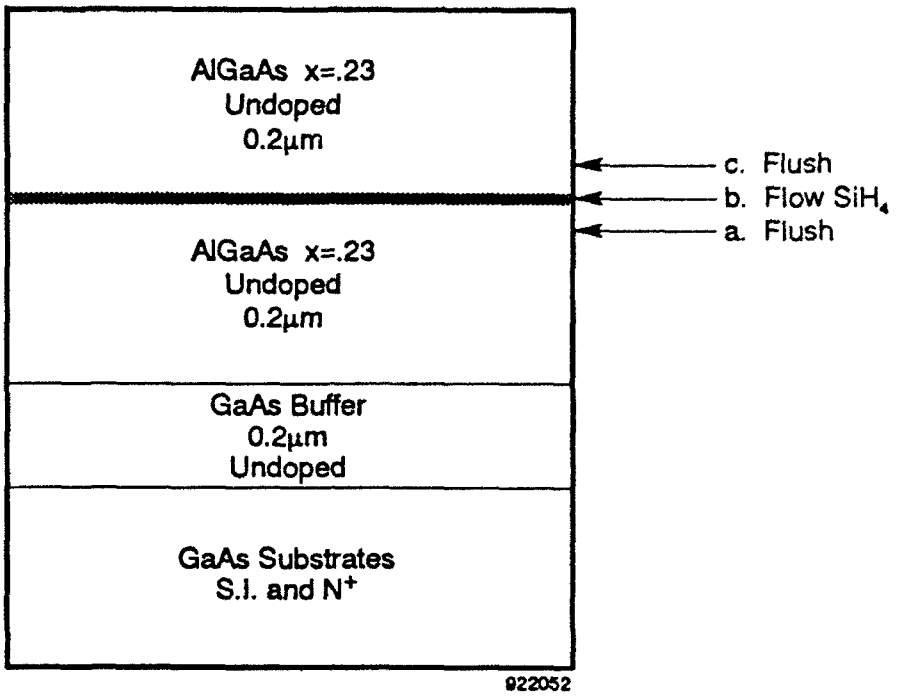

Figure 15 *Test structure for delta-doping of $Al_{0.25}Ga_{0.75}As$.*

Table I *Conditions for deposition of Δ-doped barrier layer.*

Growth temperature	650°C
Pressure	53 torr
Main flow	5 slpm
TMAl temperature	+17°C
TMGa temperature	+10°C
Growth rate	2Å/sec
AsH_3 flow	46 sccm
TMAl flow	4 sccm
TMGa flow	8 sccm
SiH_4 tank conc.	100 ppm
SiH_4 flow	25 sccm
Pre-deposit flush	15 sec
Δ-doped deposit	80 sec
Post-deposit flush	15 sec
V/III ratio	90

The growth process was as follows. After deposition of a 200 nm GaAs buffer layer on the semi-insulating substrate, 200 nm of $Al_{0.23}Ga_{0.77}As$ was grown. The flows of TMGa and TMAl were stopped, stopping growth; after a 5 second flush under arsine overpressure, the flow of SiH_4 was started. The doping of the stabilized AlGaAs surface continued for 80 seconds. The flow of SiH_4 was then terminated, followed by another 5 second flush; TMGa and TMAl were re-introduced, and growth resumed. The photoluminescence spectrum of the AlGaAs (Figure 16) shows that the aluminum content is 23.3%, which demonstrates our excellent control of composition. Polaron capacitance-voltage profiling (Figure 17) gives the expected electrical behavior.

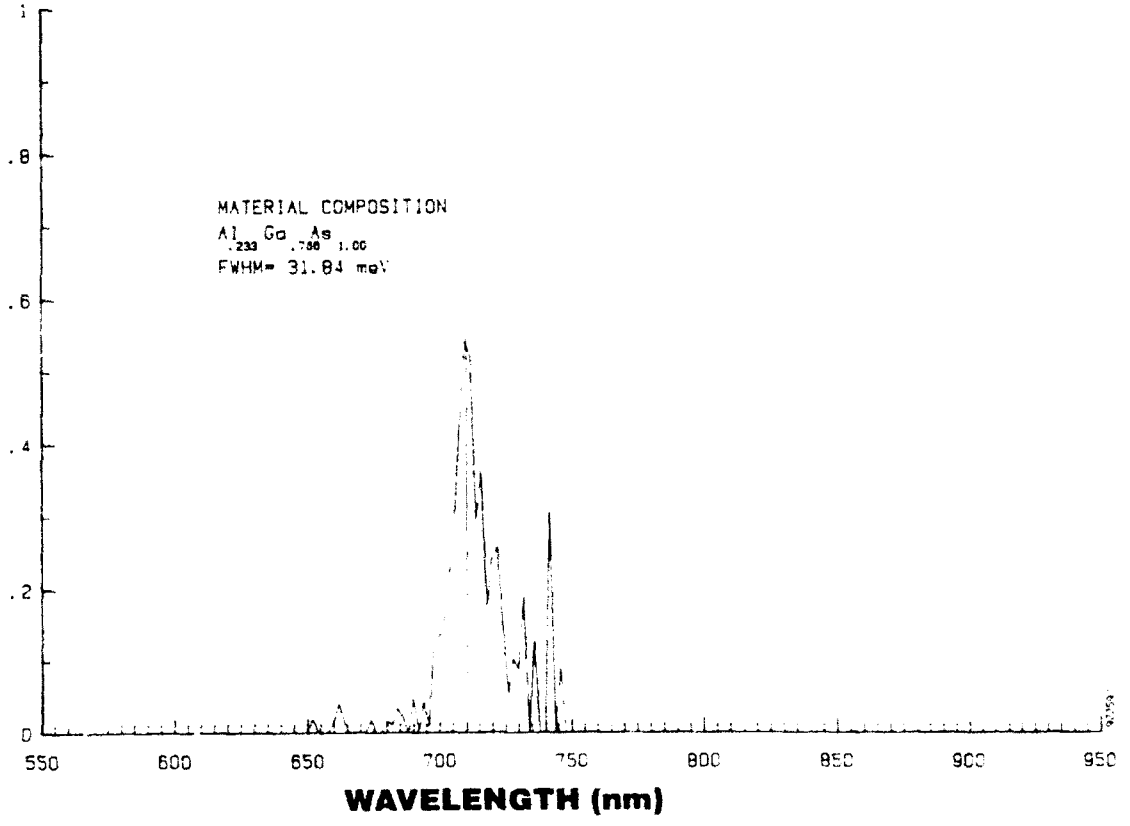

Figure 16 *Photoluminescence of Δ-doped AlGaAs layer.*

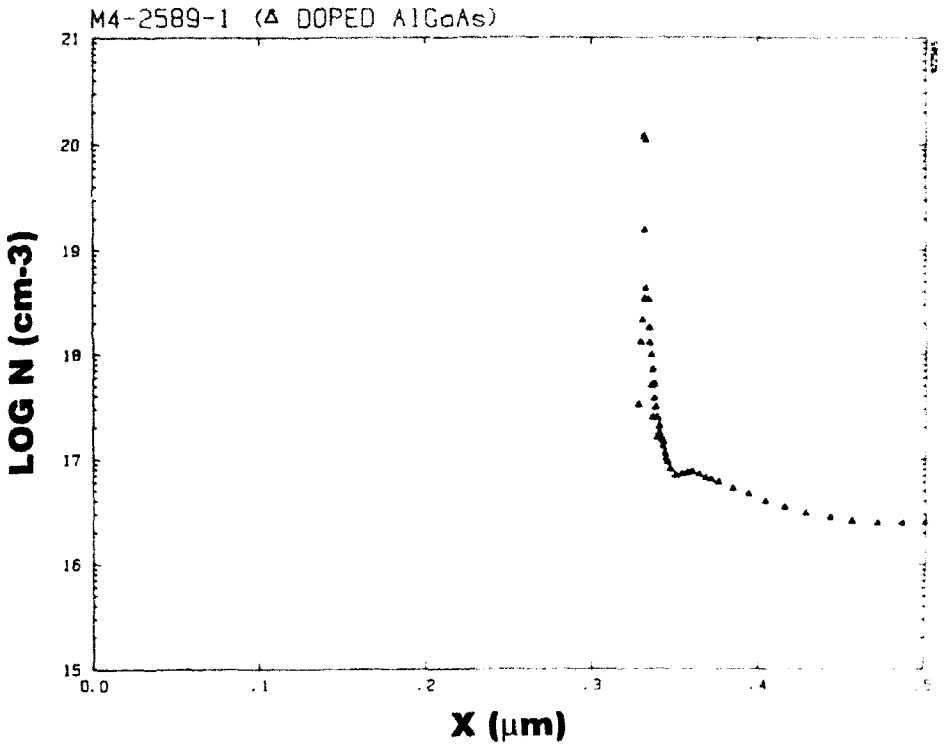

Figure 17 *Electrical characteristics of Δ-doped AlGaAs layer.*

3.5 Task 5 - Fabrication and Initial Characterization of LEFIR Reflectance Modulator

Once the properties of the individual components of the modulator had been established, structures were deposited in which all of the required semiconductor layers were sequentially grown in a single run. Wet chemistry was used to define mesas by etching all of the way down to the substrate. At this point, the thin insulator film (~3000Å of Si_3N_4) and the metal contacts (500Å of CrAu) were applied by vacuum evaporation.

Many mesas were defined and processed into modulator elements. Because of gradual variations in the epitaxially grown structure, the passbands of the individual devices ranged from 900 nm to 970 nm; see the reflectance spectra of Figure 18. Since the longer wavelength would be preferable, in order to improve transmission through the substrate by moving further from the GaAs absorption edge, the 970 nm - passband device of Figure 18 (b) was selected for further characterization.

The lack of deep reflectance minima at the Fabry-Perot modes in Figure 18 is an artifact of the monochromator measurement. It has been recognized recently that monochromators do not have sufficient resolution to fully reveal the extremely narrow transmission bands of these semiconductor etalons.[18] This was confirmed by Professor Faquir Jain of the University of Connecticut, who repeated the reflectance characterization of our modulator element, using his monochromator, and obtained a spectrum essentially identical to that of Figure 18 (b).

The currently favored technique for characterizing the Fabry-Perot modes is the measurement of per cent transmission, using a tunable Ti:sapphire laser as the light source.[19,20]

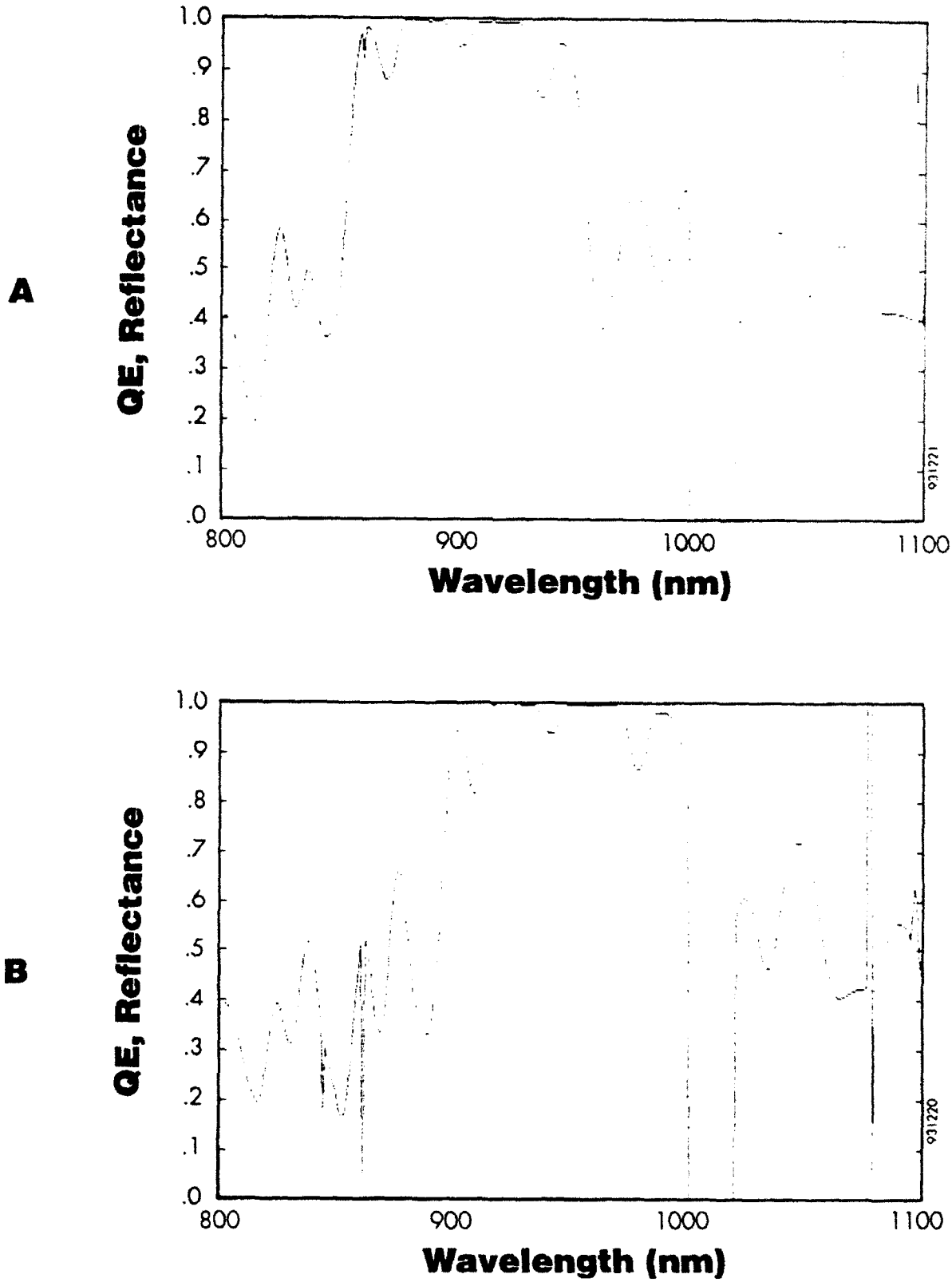

Figure 18 *(a) Reflectance spectrum for etalon with passband entered at 900 nm. (b) Reflectance spectrum for etalon with passband centered at 970 nm.*

Figure 19 shows the transmission spectrum of our modulator element. (This measurement was performed by Professor Jain's group with a tunable Ti:sapphire laser at the United Technology Research Center.) Note the extreme narrowness of the passband at 969 nm; the corresponding semilogarythmic plot of Figure 20 indicated that the transmission of the etalon changes by three orders of magnitude as the wavelength is shifted from 950 nm to 969 nm. Although an excellent result, the modulator element will be optimized in Phase II to give a peak transmission significantly greater than the measured 40%.

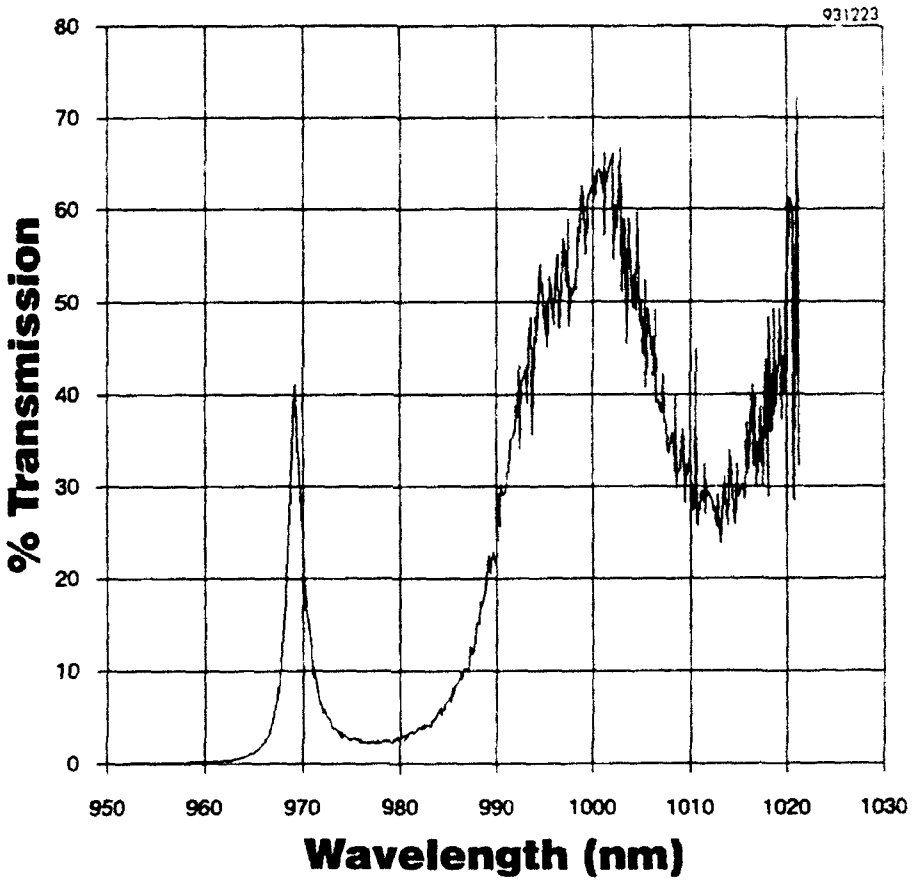

Figure 19 *Transmission through the etalon of Figure 18(b) indicating a Fabry-Perot mode at 969 nm. The broad bands at the longer wavelengths are instrumental artifacts.*

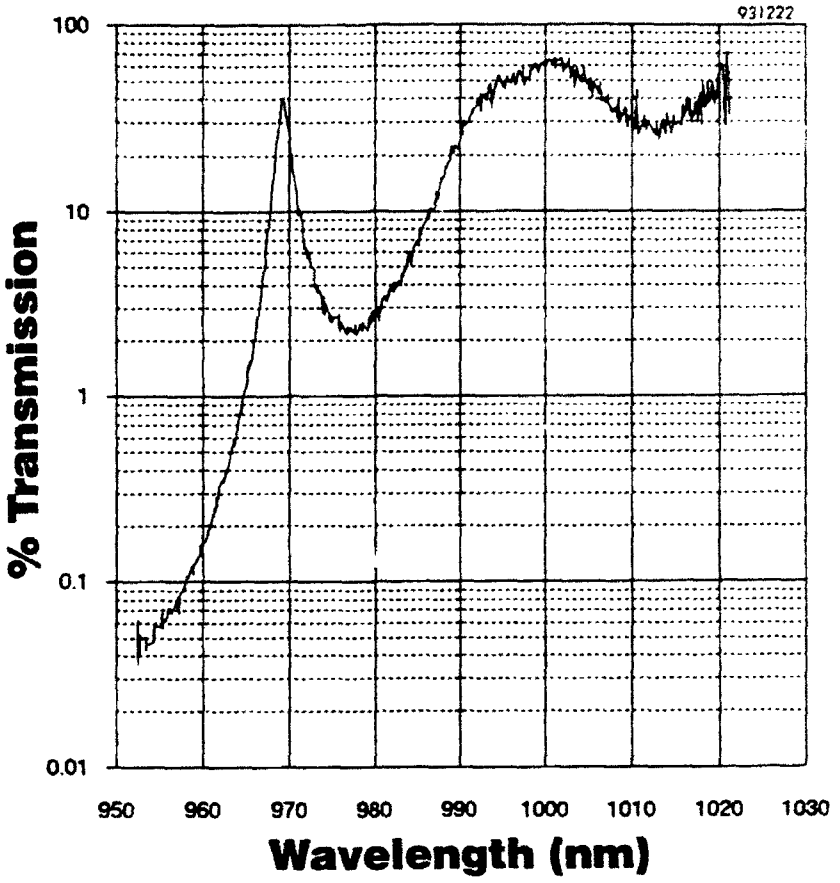

Figure 20 *The transmission changes by a factor of one thousand as the wavelength is shifted from 950 to the Fabry-Perot mode at 969 nm.*

Finally, the tunability of the proposed LEFIR modulator will be demonstrated by measuring the passband wavelength as a function of the applied voltage. It is expected that the passband will shift to longer wavelengths as the increasing electric filed sweeps electrons out of the quantum wells and thus increases the refractive index of the active region. The calculated tuning response for several values of induced Δn is given in Figure 21. The actual measurements are to be performed by Prof. Jain's group. At present, our device is in queue at the Ti:sapphire laser facility; the results will be submitted as an addendum to this report immediately upon receipt.

Figure 22 shows a two-dimensional array of modulators of various sizes. The mesas are too small to be seen without further magnification; only the metal contact pads are visible. Figure 23 is the photomicrograph of a single modulator element, emphasizing the disparity in size between the metallization and the device. At even higher magnification, Figure 24, the 20 μm x 20 μm mesa is visible. Figure 25 is the photograph of the device selected for characterization, after mounting on a header, with wiring in place. This is the modulator currently awaiting measurement for the demonstration of tunability.

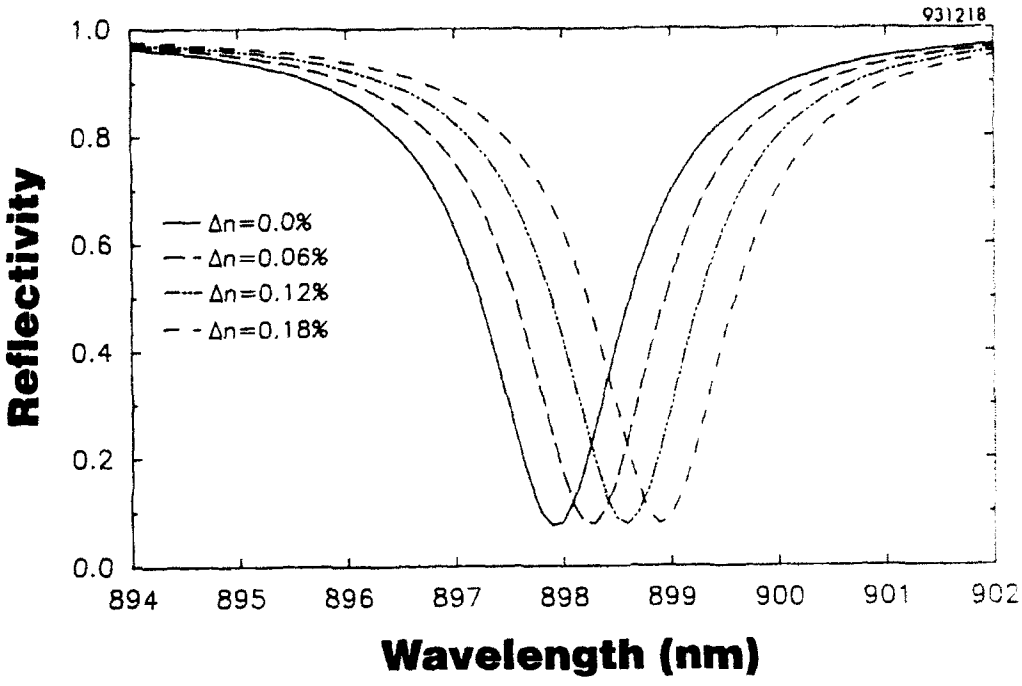

Figure 21 *Calculated tuning range of LEFIR modulator.*

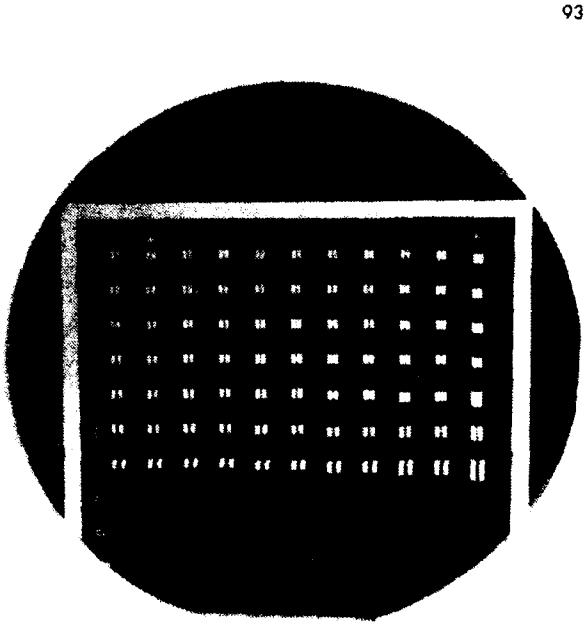

Figure 22 *Two dimensional array of modulators of various sizes.*

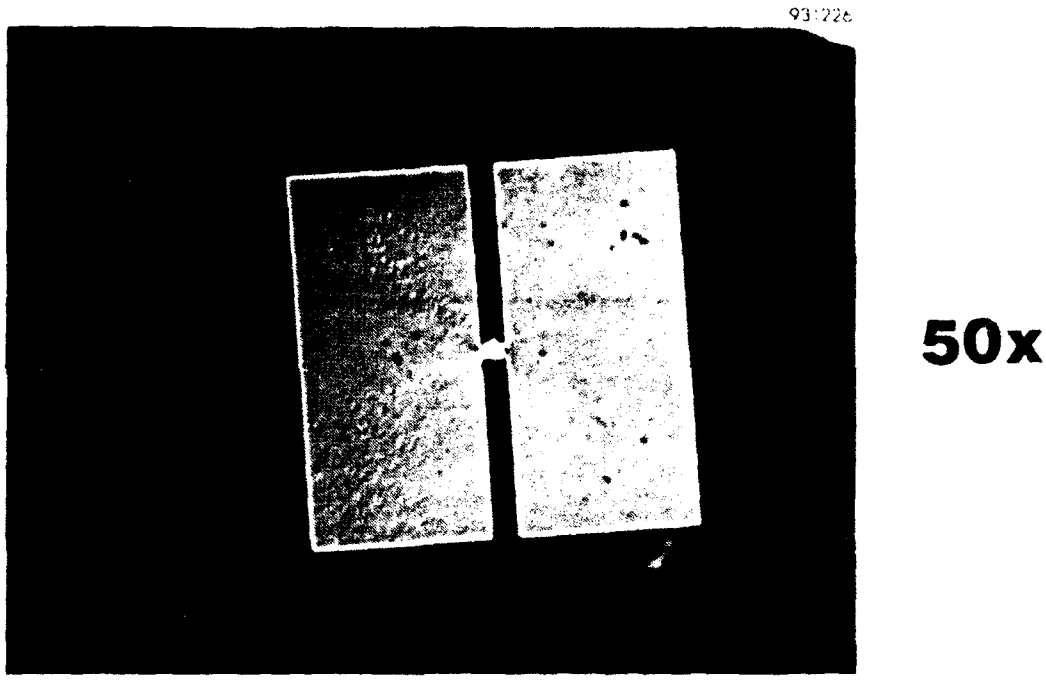

Figure 23 *Single modulator element at 50X.*

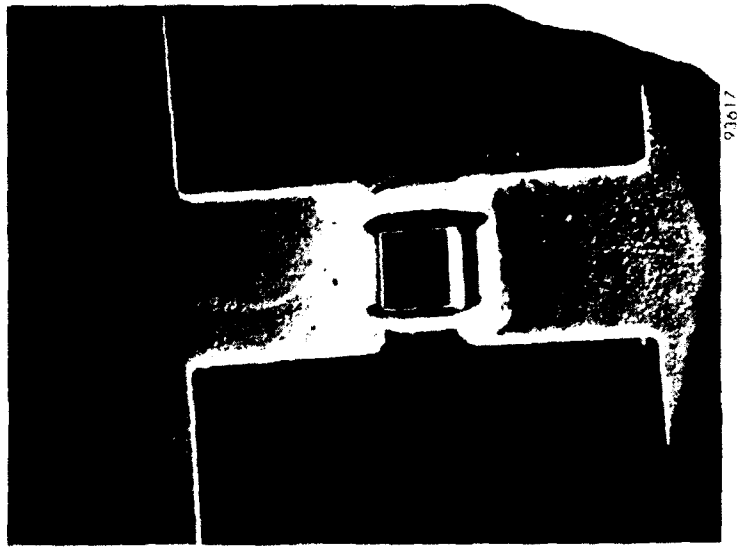

Figure 24 *Photomicrograph of modulator mesa.*

Figure 25 *Modulator mounted on header, with wiring in place.*

3.6 Task 6 - Assessment of Problem Areas and Definition of Directions for Phase II Effort

Design Refinement - The number of periods in the multi-quantum-well structure and the sheet concentration of dopants in the Δ-doped layers should be varied to maximize the refractive-index change induced by the applied voltage. The number of periods in the distributed Bragg reflectors should be increased to achieve optimal finesse (maximum reflectance and minimal bandpass width) consistent with temperature effects. The transmission at the bandpass wavelength should be maximized; although the 40% transmission at 969 nm achieved in Phase I is excellent, the Phase II goal should approach 100%. The contrast (ON/OFF) ration should be analyzed and, if desirable, improved.

Design Modification - The baseline design addresses a single-element intensity modulator for optical communications. However, there are many potential applications for the LEFIR modulator, each of which imposes specific requirements and constraints. Several of the most promising applications should be identified and the concomitant design modifications assessed. Examples include a channel demultiplexer for optical communications and a monolithic tunable diode laser; in two-dimensional arrays, a spatial light modulator (*e.g.*, for pattern recognition) and, combined with VCSELs, a self-luminous spatial light modulator.

Fabrication Improvement - There are two shortcomings of the modulator, as presently fabricated, which should be corrected. First, the large size of the contact pads precludes high-density packing of the modulator in two-dimensional arrays; a scheme for minimizing the metal area and for addressing individual modulators will be presented in the Phase II proposal. Second, the thick Si_3N_4 insulator layer induces too much capacitance, which limits the response speed; there follows and analysis of capacitance/voltage considerations that will be continued in Phase II.

Consider a modulator element with dimension of 10 μm square, as shown in Figure 26. Consider a single barrier/quantum well period, with the barrier containing 1×10^{12} charges/cm^2 in a delta-doped atomic layer. The period is 30 nm (20 nm barrier, 10 nm quantum well). Thus, the charge density per period is 3.3×10^{17} charge/cm^3. In a modulator element, we have provided 70 periods of charge control. Therefore, the total height of the mesa containing the free charge is 2.1×10^{-4} cm, and the volume containing the change is

$$\begin{aligned} V &= (10^{-3}cm \times 10^{-3}cm)\ (2.1 \times 10^{-4}cm) \\ &= 2.1 \times 10^{-10}cm^3 \end{aligned} \tag{4}$$

Thus the total number of changes present

$$\begin{aligned} Q &= (3.3 \times 10^{17}\ charge/cm^3)\ (2.1 \times 10^{-10}\ cm^3) \\ &= 6.9 \times 10^{7}\ charge \\ &= 1.1 \times 10^{-11}\ coul \end{aligned} \tag{5}$$

When the charges are moved to the side of the quantum well, we take the model shown in Figure 27. Here to make the problem tractable, we consider the electrons to be positioned at the edge of the quantum in the formation of a right circular cylinder (as shown in Figure 27). This cylinder of change is separated from the metal counter-electrode by the insulator at thickness S. The change cylinder has diameter R. It is well known[21] that the capacitance per unit length of a cylinder above a conducting plane is given by

$$\frac{C_i}{L} = \frac{2\pi\epsilon\epsilon_0}{\cosh^{-1}\left(\frac{S+R}{R}\right)} \tag{6}$$

Let S = 360 nm (the Si_3N_4 we deposited) and R = 10 nm is the radius of the stored charge. Recall that L = 10 μm = 10^{-3}cm. Then for Si_3N_4, ε = 7.5, and therefore Ci = 9.7 x 10 coul/V. Since there are 70 quantum wells in parallel, the total capacitance C_T is given by,

$$C_T = 6.7 \times 10^{-14}\ coul/V \tag{7}$$

Thus to store 1.1×10^{-11} coul will require about 162V.

Clearly, a great decrease in voltage could be accomplished by using a thinner insulator with higher dielectric constant. For example, TiO_2 has ε = 140, and for a 200 nm thick film C=7.0×10^{-13} whereupon V = about 15 volts.

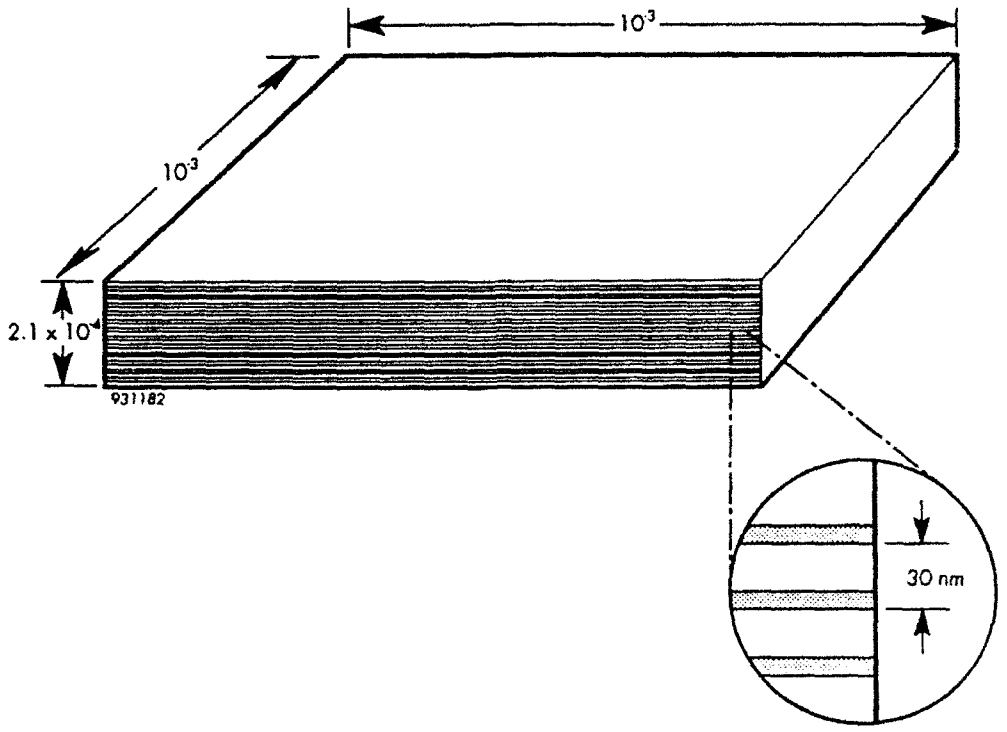

Figure 26 *Dimension of LEFIR modulator element.*

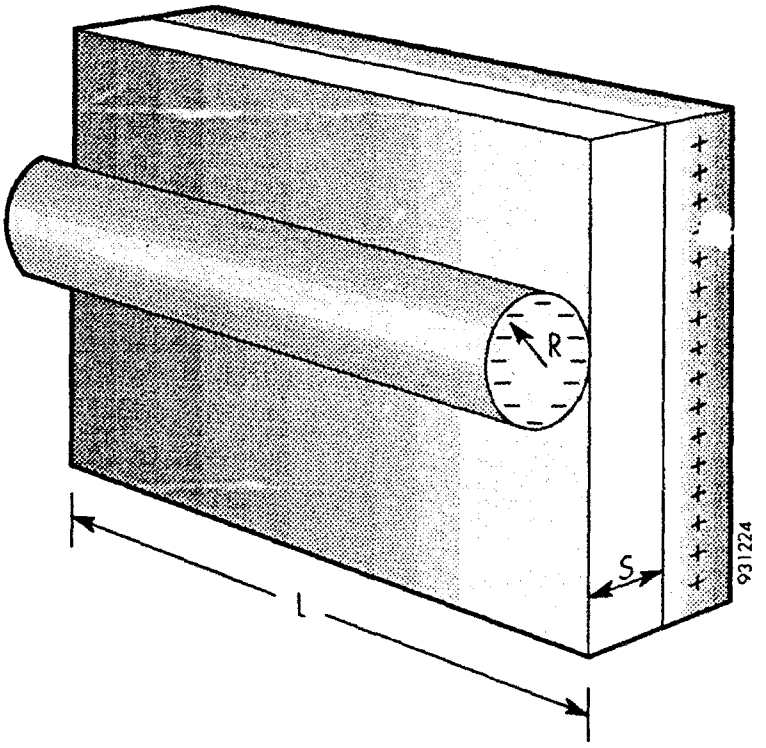

Figure 27 *Representation for calculating capacitance of modulator element.*

4 SUMMARY AND SIGNIFICANT PHASE I ACCOMPLISHMENTS

We have successfully accomplished the stated objectives of the Phase I program; *viz.*,

- the preliminary design for the LEFIR phase-shift modulator
- the fabrication and testing of the several components of the device
- the monolithic growth of the complete modulator structure, its processing into a device, and the initial evaluation of its properties

We have also answered the specific questions bearing on the feasibility of the proposed innovation:

- the several device components (distributed Bragg reflectors, quantum wells, and Δ -doped barriers) each functions as required
- under zero-bias conditions, the reflectance of the completed etalon varies with the incident wavelength to give a sharply peaked Fabry-Perot mode with an extremely narrow transmission band and high (40%) transmission
- the application of a lateral electric field is calculated to change the reflectivity of the device from 10% to 90%; the corresponding measurements are to be performed shortly

5 REFERENCES

1. J.G. Mendoza-Alverex, *et. al.*, J. Lightwave Technol. 6, 793 (1988.
2. H. Sakaki, *et. al.*, J. Applied Phys., 26, L1104 (1987).
3. R.H. Yan, R.J. Simes, L.A. Coldren, IEEE Phot. Technol. Lett., 1, 273 (1989).
4. R.H. Yan, R.J. Simes, L.A. Coldren, IEEE Phot. Technol. Lett., 2, 118 (1990).
5. J.P. van der Ziel and M. Ilegems, "Multilayer GaAs-$Al_{0.3}Ga_{0.7}$ Dielectric Quarter Wave Stacks Grown By Molecular Beam Epitaxy," Appl. Optics 11, 2627 (1975).
6. R.L. Thornton *et. al.*, "High Reflectivity GaAs-AlGaAs Mirrors Fabricated by Metalorganic Chemical Vapor Deposition," Appl. Phys. Lett. 45, 1028 (1984).
7. K. Ploog, M. Hauser, A. Fischer, Appl. Phys., A45 233 (1988).
8. K. Ploog, J. Cryst. Growth, 81, 304 (1987).
9. J.I. Pankove, Optical Processes in Semiconductors, Prentice-Hall, 39 (1971).
10. M. Wegener *et. al.*, "Absorption and Refraction Spectroscopy of a Tunable Electron Density Quantum Well and Reserve Structure," Phys. Rev. B 41, 3097 (1990).
11. M. Shur, Physics of Semiconductor Devices, Prentice Hall, 420 (1990).
12. K. Kajiyama, Y. Mizushima, S. Sakata, "Schottky Barrier Height of n-In_xGa_{1-x} Diodes," Appl. Phys. Lett., 23, 458 (1973).
13. T.H. Wood, *et. al*, "High Speed Optical Modulation with GaAs/GaAlAs Quantum Wells," Appl. Phys. Lett. 44, 16 (1984).
14. J.G. Mendoza-Alverez, F.D. Nunes, N.B. Patel. J. Appl. Phys., 51, 4365 (1980).
15. C.H. Henry. R.A. Logan, K.A. Bertness, J. Appl. Phys., 52, 4457 (1981).

16. J.E. Zucker *et. al.*,"Large Refractive Index Changes in Tunable-Electron-Density InGaAs/InAs Quantum Wells," IEEE Phot. Tech. Lett., 2, 29 (1990).
17. M.K. Chin, T.Y. Chang, W.S.C. Chang, IEEE J Quantum Electronics, 28, 2596 (1992).
18. L.A. Coldren, private communication.
19. F. Jain, private communication.
20. R.H. Yan, *et. al.*, Appl. Phys. Lett., 56, 1626 (1990).
21. M. Zahn, Electromagnetic Field Theory, J. Wiley NY, 101-103 (1979).